Relaxation dynamics of ethanol and N-butanol in diesel fuel blends from terahertz spectroscopy

Patino Camino, Rayda; Cova Bonillo, Alexis; Rodríguez-Fernández, José; Iglesias, Teresa P.; Lapuerta, Magín

DOI:
10.1007/s10762-021-00807-5

Journal of Infrared, Millimeter, and Terahertz Waves (2021) 42:772–792
https://doi.org/10.1007/s10762-021-00807-5

Relaxation Dynamics of Ethanol and N-Butanol in Diesel Fuel Blends from Terahertz Spectroscopy

Rayda Patiño-Camino[1] · Alexis Cova-Bonillo[1] · José Rodríguez-Fernández[1] · Teresa P. Iglesias[2] · Magín Lapuerta[1]

Received: 14 October 2020 / Accepted: 11 August 2021 / Published online: 30 August 2021

Abstract
Binary blends of ethanol-diesel, n-butanol-diesel, ethanol-biodiesel, and n-butanol-biodiesel have been analyzed with terahertz time-domain spectroscopy in a full range of concentrations and at room temperature. The real and imaginary parts of the complex dielectric constant of the blends were obtained from the spectra and fitted to the Debye model at low volume concentrations (up to 7.5% for ethanol in diesel and up to 20% for butanol in diesel, ethanol in biodiesel, and butanol in biodiesel blends), considering the number of relaxation processes recommended in the literature for each pure component (single for diesel, double for biodiesel, and triple for alcohols). The results indicate that the faster relaxation time in low alcohol mixtures is longer than in pure alcohols. This relaxation time increases as the alcohol content increases. The excess of the real and of imaginary parts of the dielectric constant were individually determined. The analysis of such excess and of its different contributions (volume, contrast, and interactions) suggests that the intermolecular interactions between the different components of the blends dominate the relaxation dynamics in each pseudo-binary system. Ethanol was found to move blends further away from ideal behavior than n-butanol. In fact, these latter blends showed the most ideal behavior, suggesting that the length of the alcohol carbon chain plays an important role. This information allows a possible link between the nonlinear behavior of the physicochemical properties of the blends (e.g., viscosity and surface tension) and the molecular interactions between their constituent molecules. This relation could have direct application for monitoring the fuel composition and quality in the vehicle control systems.

Keywords Biofuels · Alcohols · Debye relaxation · Dielectric constant · Loss factor · Permittivity

✉ Magín Lapuerta
Magin.Lapuerta@uclm.es

[1] Escuela Técnica Superior de Ingeniería Industrial, Edificio Politécnico, Universidad de Castilla-La Mancha, Avda. Camilo José Cela S-N, 13071 Ciudad Real, Spain

[2] Departamento de Física Aplicada, Facultad de Ciencias, Universidad de Vigo, 36200 Vigo, Spain

1 Introduction

In recent years, the use of alcohols (firstly ethanol [1] and more recently n-butanol [2]) as additives or even as components in conventional fuels (diesel, gasoline, etc.) has gained interest [3]. The reason has been widely discussed in the literature: sustainable and renewable production [4, 5], oxygen content, improvement of physical properties (e.g., viscosities, cold flow properties) [6–8], reduction of particulate emissions [9–12], etc. However, the effects on physical properties are far from being proportional to the alcohol content since many of these properties are affected by intermolecular interactions. In this context, an improved knowledge of the optical and dielectric properties of these fuels and their mixtures is interesting because they are related to the nonlinearities in some properties of relevance for internal combustion engines [13, 14]. An additional possibility is their use as onboard indicators of the fuel quality [15] and the presence of impurities [16, 17] and as quality control indicators on production and blending processes [18].

The best accepted phenomenological description of the complex frequency-dependent dielectric constant of liquid polar molecules is based on the Debye interpretation [19]. This model assumes liquids as an elastic continuum where spherical molecules (for simplicity) are dispersed and subjected to unconstrained isotropic Brownian motion, all of them with a same time constant, known as the time of relaxation. This relaxation time, τ, is often cited as the time-dependent response of such a system to a specific external excitation. In dielectric analysis, relaxation time is defined as the time required for the moments (which can be depicted by an electric displacement vector $D(t)$) to return to an aleatory distribution after the electric field ($E(t)$) has been removed. Lee [20] refers to it as a delayed response by a dielectric medium to an applied electric field. This produces a phase difference between D and E, which implies an irreversible degradation of the Gibbs free enthalpy. The rigorous mathematical approach of this model and its resolution can be found in the literature [19–22]. The resulting equations constitute the model proposed by Debye, which allows to describe the relaxation of a polar dielectric system in a linear, isotropic, and homogeneous medium as a function of frequency, according to Eq. 1:

$$\varepsilon(\omega) = \varepsilon_\infty + \frac{\varepsilon_s - \varepsilon_\infty}{1 + i.\omega.\tau} = \varepsilon_{\text{real}}(\omega) - i\varepsilon_{\text{img}}(\omega) \tag{1}$$

where ε_s is the static dielectric constant which is obtained at very low frequency ($\omega \to 0$) and ε_∞ is the very high-frequency dielectric constant ($\omega \to \infty$) of the molecules of the tested material. For practical purposes, this (complex) equation is commonly expressed with two components:

$$\varepsilon_{\text{real}}(\omega) = \varepsilon_\infty + \frac{\varepsilon_s - \varepsilon_\infty}{1 + (\omega.\tau)^2} \tag{2}$$

$$\varepsilon_{\text{img}}(\omega) = \frac{(\varepsilon_s - \varepsilon_\infty).\omega.\tau}{1 + (\omega.\tau)^2} \tag{3}$$

The real part of the dielectric constant ($\varepsilon_{\text{real}}$) describes the difference between the driving frequency (corresponding to the electric field, E) and the response frequency (corresponding to the displacement vector, D). This is a measure of energy storage, slowing down of the radiation by matter, described by the refractive index, n. The imaginary part (ε_{img}) describes

the damping factor or the loss of energy (absorption of light, quantified by the absorption coefficient in Lambert-Beer's law).

The original Debye model has been modified to approach its behavior to the shape of the spectra of real systems, considering the observed distribution of the relaxation times. The most used Debye model derivations arise from the use of modifiable exponents (α and β), which have no physical meaning, but are phenomenologically helpful, considering the widening of the relaxation band with respect to the Debye model. It can be noticed that these derived models are reduced to the single relaxation Debye model when α=0 and β=1, which is the simplest case. The most commonly used derived models are indicated in Table 1.

As has been shown, the above models involve a single relaxation process. However, for many systems, because pure liquids naturally may exhibit more than one exciting process in a certain range of frequencies, it is also possible to find more than one relaxation event. In some cases, relaxation at the atomic scale is significant, which is typical of high frequencies (and thus short relaxation times). In some other cases, the relaxation processes of the molecules themselves must be taken into consideration, which occurs at low frequencies (and longer relaxation times). Adjustments for multiple relaxation components are also required when dynamics occur on several time scales. In such cases, the abovementioned models can be extended to take into consideration as many (in general, N) relaxation processes as necessary. A general expression which includes all the possible relaxation processes is:

$$\varepsilon(\omega) = \varepsilon_\infty + \sum_{j=1}^{N} \frac{\Delta\varepsilon_j}{\left(1 + \left(i.\omega.\tau_j\right)^{1-\alpha}\right)^{\beta}} \tag{4}$$

where $\Delta\varepsilon_j$ refers to the relative contribution of the j[th] relaxation process to the macroscopic polarization.

For some materials, even these Debye model derivations are not enough [26–28] to accurately describe these relaxation dynamics, since perturbations of some molecules affect the surrounding molecules producing resonance. This phenomenon becomes important at higher frequencies (approximately 6 THz or higher) when polar liquids become resonant rather than over-damped [29]. In these cases, it is necessary to introduce the Lorentz function to consider harmonic oscillators, so the equation above becomes:

$$\varepsilon(\omega) = \varepsilon_\infty + \sum_{j=1}^{N} \frac{\Delta\varepsilon_j}{\left(1 + \left(i.\omega.\tau_j\right)^{1-\alpha}\right)^{\beta}} + \sum_{k=1}^{M} \frac{f_k.\omega_{Lk}^2}{\left(\omega_{Lk}^2 - \omega^2 - i.\omega.\gamma_L\right)} \tag{5}$$

where M is the number of damped harmonic oscillating processes, ω_L is the resonance frequency, f is the oscillator strength, and γ_L is the damping constant. Equation 5 describes

Table 1 Most common modifications from Debye model

Model	Equation
Debye [19]	$\varepsilon(\omega) = \varepsilon_\infty + \frac{\varepsilon_s - \varepsilon_\infty}{1+i\omega\tau}$
Cole-Cole [23]	$\varepsilon(\omega) = \varepsilon_\infty + \frac{\varepsilon_s - \varepsilon_\infty}{1+(i\omega\tau)^{1-\alpha}}$
Davidson-Cole [24]	$\varepsilon(\omega) = \varepsilon_\infty + \frac{\varepsilon_s - \varepsilon_\infty}{(1+i\omega\tau)}^{\beta}$
Havriliak-Negami [25]	$\varepsilon(\omega) = \varepsilon_\infty + \frac{\varepsilon_s - \varepsilon_\infty}{\left(1+(i\omega\tau)^{1-\alpha}\right)}^{\beta}$
α,β are in the range [0,1]	

the most complete relaxation process and is complex enough to describe most of the cases. Also, different approaches have been proposed to describe the relaxation processes that cannot be fitted with this type of models [30–32]. Besides, some of these approaches have used molecular dynamics modeling [33, 34].

The practical use of Eq. 5 to model relaxation processes is far from easy. It becomes more difficult, or even impossible, as the number of parameters to be fitted increases. This is the result of the various types of relaxation processes occurring at very different frequencies and at different orders of magnitude. These include local processes of short-term duration such as the rotation/translation of molecules after the rupture of the H-bond [35, 36] and cooperative relaxation processes such as the reorientational effects of the bulk medium or of large molecular clusters [37]. The appearance of factors which may result in the change of the absorption capacity throughout the media is also possible, so that there is not a single relaxation process, but many of them overlap. This is known as relaxation time distribution [38, 39].

For instance, the dielectric spectra for alcohols (particularly for ethanol) have been found to exhibit multiple relaxation processes. Barthel and Buchner [40] reported that protic liquids (containing O-H and/or N-H bonds) showed three relaxation processes: restoration of the structure of the perturbed liquid bulk (slower process), the intramolecular rotation of individual molecules of the bulk liquid and of molecules linked by hydrogen bonds (intermediate times), and a very short relaxation time of about 1 ps. This fastest relaxation process is caused by the formation, breaking, and/or reorientation of the hydrogen bonds [35]. Barthel and Buchner [40] also demonstrated that aprotic liquids fit single relaxation Debye models because they do not contain any H-bond.

The frequency range has an influence on the selection of the number of relaxation processes for adjustment purposes. Kindt and Schmuttenmaer [29] showed that water fitted well to the double Debye model in the range 0.0009 to 0.42 THz, whereas Beneduci [41] demonstrated the existence of a third relaxation process by amplifying the frequency range up to 1 THz. Considering this, in the case of monohydric alcohols, a triple Debye model is required.

This work presents the second part of a previous study [42], in which optical and dielectric properties were obtained for ethanol or n-butanol blends in diesel-type fuels using terahertz time-domain spectroscopy (TDS-THz) [43]. In this previous paper, spectra of the absorption coefficient and refractive index of the mixtures were calculated, and from these, spectra of the real and imaginary parts of the complex dielectric constant (also called relative permittivity) were determined. In this second part, the effect of mixing on molecular dynamics is evaluated.

2 Material and Methods

2.1 Materials

The following fuels were used in this work: diesel fuel (supplied by the Spanish company Repsol), biodiesel (supplied by the Spanish company Bio Oils), ethanol (donated by Abengoa Bioenergy), and n-butanol (supplied by Green Biologics Ltd.). The diesel composition was 30.66% paraffins, 44.61% naphthenes, and 23.76% aromatics, without any oxygen content, and complied with standard EN 590. The fatty acid composition of biodiesel (produced from 80% soybean oil and 20% palm 20 and complied with standard EN 14214) was 47.26% linoleic (C18:2), 26.22% oleic (C18:1), 15.67% palmitic (C16:0), 5.39% α-linoleic (C18:3),

and 3.77% stearic (C18:0) esters, determined using gas chromatography, as established in method EN 14103. The methanol content in this biodiesel was found to be under 0.15% (m/m), which is below the limit specified in EN 14214, which is 0.2% (m/m). More detailed diesel and biodiesel compositions, as well as the main properties of base fuels and pure alcohols used for blends, have been published previously [42].

Samples were prepared for ethanol-diesel, n-butanol-diesel, ethanol-biodiesel, and n-butanol-biodiesel in pseudo-binary mixtures, with special focus on low alcohol concentration blends since high alcohol blends in diesel engines are unfeasible in practice [6, 7, 44–46]. Consequently, the samples were prepared at room temperature (around 25 °C) containing 0, 2.5, 5.0, 7.5, 10, 15, 20, 40, 60, 80, 90, and 100% (v/v) of alcohol in the base fuel. Regarding ethanol/diesel blends, the test matrix was restricted by the limited miscibility of 10–80% of the alcohol content at the operating temperature [6]. This way, Bu10-B denotes 10% (v/v) n-butanol and 90% (v/v) biodiesel (note that for simplicity the "n" for n-butanol is omitted for these purposes). The same nomenclature was followed for the samples as in the preceding article [42].

2.2 Experimental Setup

The main equipment used to perform this work, a THz time-domain spectrometer, was described previously [42]. Briefly, it includes a femtosecond Ti:sapphire laser, which generates ultra-short pulses (60–80 fs) with a frequency of 80 MHz and an average output power of about 650 mW. Two photoconductive low-temperature gallium-arsenic (LT-GaAs) antennas were used for emission and detection of THz radiation. The power emitted from THz radiation was approximately 10 μW. The emitted power depends on the pumping power, and it is measured using a calibrated photoconductive antenna. Silicone lenses were attached to the antennas for better efficiency. Aluminum-coated parabolic mirrors were used to collimate the THz beam from the emitter through sample until the detector. The sample cell was a 2-mm optical path quartz cuvette, based on previous works [47, 48]. The cell temperature was controlled at around 25°C through the control of room temperature. The spectra were collected in transmission mode.

The static relative dielectric constant, for all the pure fuels, was measured in the laboratory using a homemade cell consistent of a parallel plate condenser (with radius = 8 cm) sandwiching a 3-mm-thick dielectric material. Also, a digital multimeter Peak Tech 2005 at 100 Hz was used for the capacitance measurement of the cell without and with sample.

2.3 Summary of Data Processing

Figure 1 shows a scheme summarizing the processing of the spectra obtained from pure fuels (ethanol, n-butanol, diesel, and biodiesel) and their binary blends (not shown in the figure). As explained by Beneduci [42], each sample was analyzed to obtain (I) the pulse by TDS-THz. Every time-domain spectrum, $E_j(t)$, was preprocessed according to the conceptual framework proposed by Zhang et al. [49] and used by other researchers [26, 47, 48]. Fast Fourier transform (FFT) was applied (II) to each temporal waveform in order to obtain the amplitude $A_j(\omega)$ and phase $\theta_j(\omega)$. With Fresnel equations and using the air in the empty cell as reference, the frequency-dependent real part of the refractive index, $n_j(\omega)$, and the absorption coefficient, $\alpha_j(\omega)$, were determined (III) for each sample. Finally, from these, the real and the imaginary parts of the complex dielectric constant $\varepsilon_{\mathrm{real}j}(\omega)$ and $\varepsilon_{\mathrm{img}j}(\omega)$ were also determined (IV). From

the latter, two theoretical approaches are presented in this work: the first part presents the modeling of the dielectric constant for the low alcohol concentrations. The second part shows an analysis of the effect of mixing alcohols with diesel-type fuels, based on the excess of the real and imaginary parts of the dielectric constant.

3 Results and Discussion

3.1 Model Fitting for Pure Liquids

Based on the above, triple Debye models were tested to simulate the relaxation process of ethanol and n-butanol. For both diesel and biodiesel, various steps of relaxation were tested. In the case of diesel, a single Debye model was found to be enough for fitting, which coincides with Arik et al. [47] and Barthel and Buchner [40]. In contrast, biodiesel required double Debye model for the adjustment of the experimental data. Table 2 shows the equations resulting from the expansion of Eq. 1 for all pure fuels.

Likewise, harmonic oscillators were not included, based on the non-existence of absorption bands in the studied range, neither for ethanol, extensible to n-butanol, nor for gasoline, extensible to diesel and biodiesel [29, 40]. The molecular resonance leading to such absorption bands is more important at much higher frequencies than those considered in this work [20]. As an example, parameter such as τ_{1B} should be understood as the first relaxation time for pure biodiesel, and the same applies for the equivalent parameters.

Hence, the adjustment consists in determining each parameter for each mixture of alcohol (Et or nBu) and base fuel (D or B). As an example, for pure ethanol, seven parameters ($\varepsilon_{\infty Et}$, ε_{1Et}, ε_{2Et}, ε_{3Et}, τ_{1Et}, τ_{2Et}, τ_{3Et}) must be fitted.

The adjustment strategy used was to simultaneously minimize the sum of the mean squared deviations (MSD) between the experimental and modeled values of the real and imaginary parts of the complex dielectric constant to an acceptable low value (MSD<0.001) by using a

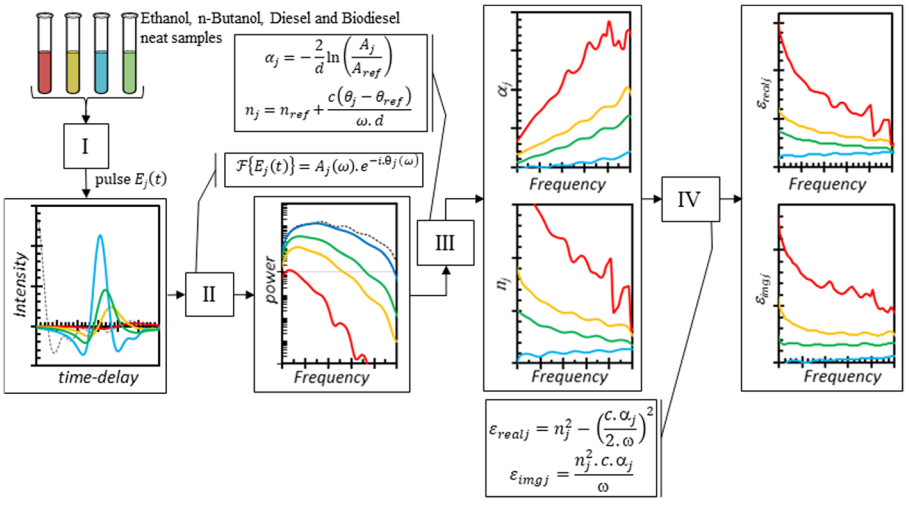

Fig. 1 Methodology used to determine the complex dielectric constant starting from the spectra obtained by TDS-THz for pure fuels (ethanol, n-butanol, diesel, and biodiesel)

Table 2 Expansion of the real and imaginary parts of the Debye dielectric relaxation model for diesel, biodiesel, ethanol, and n-butanol

Diesel	$\varepsilon_{\text{real } D}(\omega) = \varepsilon_{\infty D} + \frac{\varepsilon_{1\ D} - \varepsilon_{\infty D}}{1+(\omega.\tau_{1\ D})^2}$
	$\varepsilon_{\text{img } D}(\omega) = (\varepsilon_{1\ D} - \varepsilon_{\infty D}) \frac{\omega.\tau_{1\ D}}{1+(\omega.\tau_{1\ D})^2}$
Biodiesel	$\varepsilon_{\text{real } B}(\omega) = \varepsilon_{\infty B} + \frac{\varepsilon_{1\ B} - \varepsilon_{2\ B}}{1+(\omega.\tau_{1\ B})^2} + \frac{\varepsilon_{2\ B} - \varepsilon_{\infty B}}{1+(\omega.\tau_{2\ B})^2}$
	$\varepsilon_{\text{img } B}(\omega) = (\varepsilon_{1\ B} - \varepsilon_{2\ B}) \frac{\omega.\tau_{1\ B}}{1+(\omega.\tau_{1\ B})^2} + (\varepsilon_{2\ B} - \varepsilon_{\infty B}) \frac{\omega.\tau_{2\ B}}{1+(\omega.\tau_{2\ B})^2}$
Ethanol	$\varepsilon_{\text{real Et}}(\omega) = \varepsilon_{\infty \text{Et}} + \frac{\varepsilon_{1\text{Et}} - \varepsilon_{2\text{Et}}}{1+(\omega.\tau_{1\text{Et}})^2} + \frac{\varepsilon_{2\text{Et}} - \varepsilon_{3\text{Et}}}{1+(\omega.\tau_{2\text{Et}})^2} + \frac{\varepsilon_{3\text{Et}} - \varepsilon_{\infty\text{Et}}}{1+(\omega.\tau_{3\text{Et}})^2}$
	$\varepsilon_{\text{img Et}}(\omega) = (\varepsilon_{1\text{Et}} - \varepsilon_{2\text{Et}}) \frac{\omega.\tau_{1\text{Et}}}{1+(\omega.\tau_{1\text{Et}})^2} + (\varepsilon_{2\text{Et}} - \varepsilon_{3\text{Et}}) \frac{\omega.\tau_{2\text{Et}}}{1+(\omega.\tau_{2\text{Et}})^2} + (\varepsilon_{3\text{Et}} - \varepsilon_{\infty\text{Et}}) \frac{\omega.\tau_{3\text{Et}}}{1+(\omega.\tau_{3\text{Et}})^2}$
N-Butanol	$\varepsilon_{\text{real Bu}}(\omega) = \varepsilon_{\infty\text{Bu}} + \frac{\varepsilon_{1\text{Bu}} - \varepsilon_{2\text{Bu}}}{1+(\omega.\tau_{1\text{Bu}})^2} + \frac{\varepsilon_{2\text{Bu}} - \varepsilon_{3\text{Bu}}}{1+(\omega.\tau_{2\text{Bu}})^2} + \frac{\varepsilon_{3\text{Bu}} - \varepsilon_{\infty\text{Bu}}}{1+(\omega.\tau_{3\text{Bu}})^2}$
	$\varepsilon_{\text{img Bu}}(\omega) = (\varepsilon_{1\text{Bu}} - \varepsilon_{2\text{Bu}}) \frac{\omega.\tau_{1\text{Bu}}}{1+(\omega.\tau_{1\text{Bu}})^2} + (\varepsilon_{2\text{Bu}} - \varepsilon_{3\text{Bu}}) \frac{\omega.\tau_{2\text{Bu}}}{1+(\omega.\tau_{2\text{Bu}})^2} + (\varepsilon_{3\text{Bu}} - \varepsilon_{\infty\text{Bu}}) \frac{\omega.\tau_{3\text{Bu}}}{1+(\omega.\tau_{3\text{Bu}})^2}$

nonlinear least squares procedure. This type of multiparameter adjustment is used commonly for data analysis in spectroscopy [29, 41, 48, 50–53]. Mittleman et al. [54] pointed out that, although this procedure necessarily allows some freedom in the choice of such adjustment parameters, the requirement to simultaneously satisfy $\varepsilon_{\text{real}}$ and ε_{img} significantly reduces such freedom. In this sense, some considerations should be made to solve such problems in order to obtain a certain quality in the adjustment. A usual practice [29, 47, 48] is to take those corresponding to the slowest processes as fix values, as far as conditions, such as temperature, remain unchanged. With all this determined, it is evident that the number of parameters to be adjusted is significantly reduced. For diesel, biodiesel, and n-butanol, the values for the static relative dielectric constant, ε_1 (that is, ε_{1D}, ε_{1B}, and $\varepsilon_{1\text{Bu}}$), were taken from the experimental result. On the other hand, the values for ε_∞ (that is, $\varepsilon_{\infty D}$, $\varepsilon_{\infty B}$, and $\varepsilon_{\infty\text{Bu}}$) were taken as the horizontal asymptotic trend (frequency $\rightarrow +\infty$) using the logistic model of Origin Pro 7 software. For ethanol, however, these assumptions were not possible, probably because of the effect of water interference (expressed in a very highly fluctuating reading). For the adjustment, the ethanol spectrum had to be limited to a range 0.1 to 0.5 THz.

All adjustments were carried out using the GRG nonlinear solving method of the Solver tool in MS Excel spreadsheet. Figure 2 shows the experimental data (empty discrete symbols) and the adjustment lines according to the Debye model for diesel, biodiesel, ethanol, and n-butanol.

Table 3 lists the fitting results obtained by modeling experimental data assuming single Debye model for diesel, double Debye model for biodiesel, and triple Debye model for ethanol and n-butanol Debye relaxation processes and their comparison with some results reported in the literature. Although variations are observed between the different results, there is an acceptable consistency between the different parameters.

Pure diesel fuel, a non-hydrogen-bonded liquid (see composition), was fitted to a single Debye model, so the process only required the adjustment of τ_{1D}, resulting in 0.19 ps, higher than that reported by Arik et al. [48]. This is probably due to the difference in composition between both diesel samples. However, this value is among those expected for diesel-type mixtures [29].

For biodiesel, to the authors' knowledge, no fit to Debye model was found in the literature for comparison. This could be comprehensible, considering the variability in the composition of biodiesel fuels (esters with a variable carbon chain length around

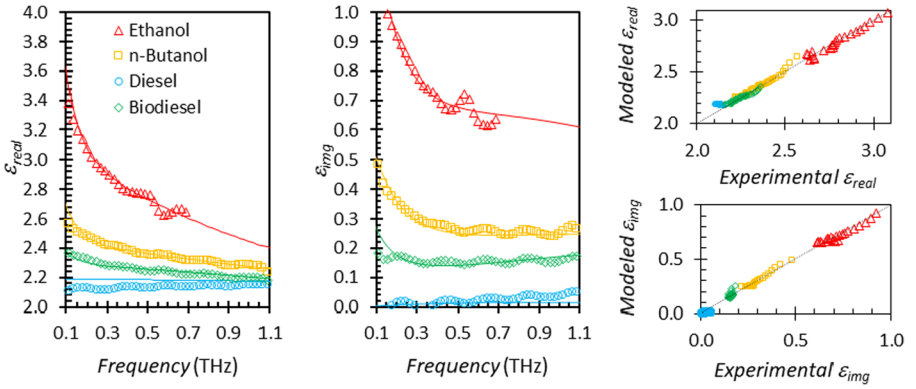

Fig. 2 Real (left) and imaginary (center) parts of dielectric constant for pure fuels. Empty symbols refer to experimental data, and solid lines refer to fitted model. Correlation between experimental and modeled values contrast, and interactions) suggest for real (top right) and imaginary (bottom right) parts

18 carbons, containing C-O-C groups and variable number of unsaturated bonds). For this reason and according to the procedure used by Arik et al. [47] (applied to gasoline), single- and double-level Debye models were evaluated. The single-level Debye model was proved not to be enough to fit the experimental data. Therefore, a double-level Debye model was selected resulting in a better fit. Accordingly, the slowest relaxation time (τ_{1B} = 3.57 ps) could be attributed to collective reorientations of clusters formed by molecules of the esters that compose the fuel, while the fastest relaxation time (τ_{2B} = 0.08 ps) could be associated with the reorientation of individual molecules.

Both alcohols were fitted, as mentioned before, to triple Debye models. A plausible explanation of these three relaxation processes is as follows: the slowest relaxation time is attributable to the re-establishment of the disturbed structure of the bulk liquid [40]. The second relaxation time corresponds to intramolecular rotation of alcohol molecules as monomers and into chains or networks linked by H-bond. The fastest

Table 3 Dielectric relaxation parameters of pure fuels as determined by fit of the data from the literature and from this work

Fuel	Source	Debye model	ε_1	ε_2	ε_3	ε_∞	τ_1 (ps)	τ_2 (ps)	τ_3 (ps)
Diesel	[48]	Single	2.16	N/A	N/A	2.14	0.10	N/A	N/A
Ethanol	[29]	Triple	24.35	4.15	2.72	1.93	161	3.3	0.22
Ethanol	[40]	Triple	24.32	4.49	3.82	2.69	163	8.97	1.81
Ethanol	[55]	Single	25.7	N/A	N/A	N/A	170	N/A	N/A
Ethanol	[52]	Triple	24.5	4.5	3.76	2.6	165	10.04	1.69
Ethanol	[53]	Triple	24.4	4.4	3.00	1.85	163	4.51	0.33
N-Butanol	[55]	Single	N/A	N/A	N/A	N/A	538	N/A	N/A
Diesel	This work	Single	2.19 [a]	N/A	N/A	2.16 [b]	0.19	N/A	N/A
Biodiesel	This work	Double	2.95 [a]	2.27	N/A	1.90 [b]	3.57	0.08	N/A
Ethanol	This work	Triple	24.35 [c]	4.75	2.83	1.93 [c]	161 [c]	1.96	0.14
N-butanol	This work	Triple	17.52 [a]	3.31	2.38	1.99 [b]	523	2.25	0.10

a: Taken as the experimental relative dielectric constant at 100 Hz

b: Estimated according to the asymptotic trend from the logistic model of Origin Pro 7 software

c: Taken from Kindt and Schmuttenmaer [29]

relaxation time (around 1 ps) is the result of the dynamics of the H-bond. For ethanol, the $\varepsilon_{\infty Et}$ value is experimental, the slowest relaxation (τ_{1Et} = 161 ps and ε_{1Et} = 24.35) was taken from the Kindt and Schmuttenmaer publication [29], while the others were determined from fitting to experimental results and are in Table 3. The second relaxation time was τ_{2Et} = 1.96 ps, and the fastest relaxation time was τ_{3Et} = 0.14 ps. The corresponding dielectric contributions (ε_{2Et} and ε_{3Et}) from each relaxation are also shown in Table 3. While it was not difficult to obtain such an adjustment for ethanol from the literature [29, 53], the same was not found for n-butanol. From Barthel and Buchner [40], data from n-propanol and n-pentanol, C3 and C5 alcohols, were taken to interpolate each parameter for n-butanol (C4 alcohol). The latter were used as seed in the fitting process.

3.2 Model Fitting for Blends

Barthel and Buchner [40] demonstrated that the dielectric relaxation behavior of a mixture is intimately related to the properties of its components. This has been corroborated by many authors [56–58]. The methodology in this work was adapted from that used by Arik et al. [48] for ethanol and gasoline blends, due to the similarity of this system with the ones discussed in this work. They used a mixing rule based on the volumetric fractions (z_j), which is consistent with that proposed by Reis and Iglesias [59] and used in other works [36]. Unlike the adjustment method of Arik et al. [48], no correction was made to compensate the deviation of the volumetric composition from the ideal one. Instead, for a blend composed of an alcohol (alc) and a base fuel (bf) with z_{alc} and z_{bf}, respectively, variable values of the dielectric constants of the components were used, leading to the following set of equations:

$$\varepsilon_{\text{real alc.bf}}(\omega) = z_{\text{bf}}\left[\varepsilon_{\text{real bf–mix}}(\omega)\right] + z_{\text{alc}}\left[\varepsilon_{\text{real alc–mix}}(\omega)\right] \tag{6 – a}$$

$$\varepsilon_{\text{img alc.bf}}(\omega) = z_{\text{bf}}\left[\varepsilon_{\text{img bf–mix}}(\omega)\right] + z_{\text{alc}}\left[\varepsilon_{\text{img alc–mix}}(\omega)\right] \tag{6 – b}$$

where $\varepsilon_{\text{real alc-mix}}$ refers to the real part of the dielectric constant of the alcohol in the corresponding alc-bf mixture. The same applies to the other factors of the system of Eqs. 6-a and 6-b. In principle, these factors (such as $\varepsilon_{\text{real alc-mix}}$) have the same form as those shown in Table 2 for pure components; however, each parameter is updated to its corresponding values in the mixture. Thus, for ethanol, instead of τ_{3Et} (third relaxation time of pure ethanol), $\tau_{3Et\text{-}EtD}$ (third relaxation time of the ethanol into an Et-D blend) was used. At first glance, the number of resulting parameters makes the resulting system of equations very difficult to be solved and requires additional assumptions. As Arik et al. [48] explained, it is expected that the most significant mixing effect will be observed in the fastest relaxation time. This is because the continuity of the hydrogen bonds on the alcohol molecules is disrupted. Based on the above, it can be assumed that only the fastest relaxation process for each component is affected by mixing. Therefore, the parameters corresponding to all other relaxation processes can be assumed unaltered.

After all these considerations, for ethanol and diesel blends (for example), replacing terms from Table 2 for each component into Eq. 6, updating the parameters corresponding to the fastest step (first for diesel and third for ethanol), the following system of equations is obtained:

$$\varepsilon_{\text{real EtD}}(\omega) = z_D\left[\varepsilon_{\infty D} + \frac{\varepsilon_{1D-\text{Et}D} - \varepsilon_{\infty D}}{1 + (\omega.\tau_{1D-\text{Et}D})^2}\right] + \\ + z_{\text{Et}}\left[\varepsilon_{\infty \text{Et}} + \frac{\varepsilon_{1\text{Et}} - \varepsilon_{2\text{Et}}}{1 + (\omega.\tau_{1\text{Et}})^2} + \frac{\varepsilon_{2Et} - \varepsilon_{3\text{Et}-\text{Et}D}}{1 + (\omega.\tau_{2\text{Et}})^2} + \frac{\varepsilon_{3\text{Et}-\text{Et}D} - \varepsilon_{\infty \text{Et}}}{1 + (\omega.\tau_{3\text{Et}-\text{Et}D})^2}\right] \quad (7-\text{a})$$

$$\varepsilon_{\text{img EtD}}(\omega) = z_D\left[\frac{(\varepsilon_{1D-\text{Et}D} - \varepsilon_{\infty D}).\omega.\tau_{1D-\text{Et}D}}{\left(1 + (\omega.\tau_{1D-\text{Et}D})^2\right)}\right] + \\ + z_{\text{Et}}\left[\frac{(\varepsilon_{1\text{Et}} - \varepsilon_{2\text{Et}}).\omega.\tau_{1\text{Et}}}{1 + (\omega.\tau_{1\text{Et}})^2} + \frac{(\varepsilon_{2\text{Et}} - \varepsilon_{3\text{Et}-\text{Et}D}).\tau_{2\text{Et}}}{1 + (\omega.\tau_{2\text{Et}})^2} + \frac{(\varepsilon_{3\text{Et}-\text{Et}D} - \varepsilon_{\infty \text{Et}}).\tau_{3\text{Et}-\text{Et}D}}{1 + (\omega.\tau_{3\text{Et}-\text{Et}D})^2}\right] \quad (7-\text{b})$$

where $\varepsilon_{\text{real EtD}}$ and $\varepsilon_{\text{img EtD}}$ correspond to the modeled real and imaginary parts and z_{Et} and z_D are the volumetric fractions for Et-D blends.

As described above, as an adjusting approach, deviations were minimized for both real and imaginary parts until MSD <0.001. It was found that by increasing the alcohol content, a point is reached where the fitting procedure does not converge so that the adjustment is not possible. Perhaps this occurs because from a certain concentration onwards, for each system, the effect of alcohol becomes more and more important, and the relaxation processes, initially taken as non-variable by the effect of mixing, turn important. A good fitting was possible for the lower alcohol concentrations for each system: up to 7.5% (v/v) for Et-D blends and up to 20% (v/v) for Et-B, Bu-D, and Bu-B blends. The results are shown and discussed below.

The results obtained by adjusting the fastest relaxation time for each alcohol ($\tau_{3\text{Et-Et}D}$, $\tau_{3\text{Bu-Bu}D}$, $\tau_{3\text{Et-Et}B}$, and $\tau_{3\text{Bu-Bu}B}$) and base fuel ($\tau_{1\text{D-EtD}}$, $\tau_{1D\text{-BuD}}$, $\tau_{2B\text{-EtB}}$, and $\tau_{2B\text{-BuB}}$) in the blends as a function of alcohol content are shown in Fig. 3. Some observations can be made. The first is the increase in relaxation time for diluted alcohols with respect to their pure state (not shown in Fig. 3 but in Table 3). The relaxation time of ethanol rises from 0.14 ps in pure form to 1.31 ps for the 2.5% (v/v) blend in diesel and up to 1.59 ps for the 2.5% (v/v) blend in biodiesel. Similarly, the relaxation time of n-butanol rises from 0.10 ps for the pure state to 2.93 ps for the 2.5% (v/v) blend in diesel and up to 1.75 ps for the 2.5% (v/v) blend in biodiesel. For contents from 2.5% (within the modeled range), the fastest relaxation times follow similar trends, but the numerical values, especially for butanol blends, fall out of the measured frequency range, and therefore, numerical values are only indicative. In pure alcohols, despite the molecules are hydrogen-bonded interlinked forming a 3D network, the relaxation times are shortest, indicating that molecules respond synchronizedly to the electric field. In the case of 2.5% (v/v) alcohol solutions, the alcohol is dispersed in the base fuel, with alcohol molecules being surrounded by dissimilar non-polar molecules (from diesel and biodiesel) without any capacity to form hydrogen bonds but with low-energy molecular interactions. However, the different stereography of such dissimilar molecules reduces the freedom of movement and therefore leads to longer relaxation times. When the relaxation times of alcohols are compared to those of the base fuels, it can be concluded that the former ones have a dominant effect on relaxation dynamics of the blends.

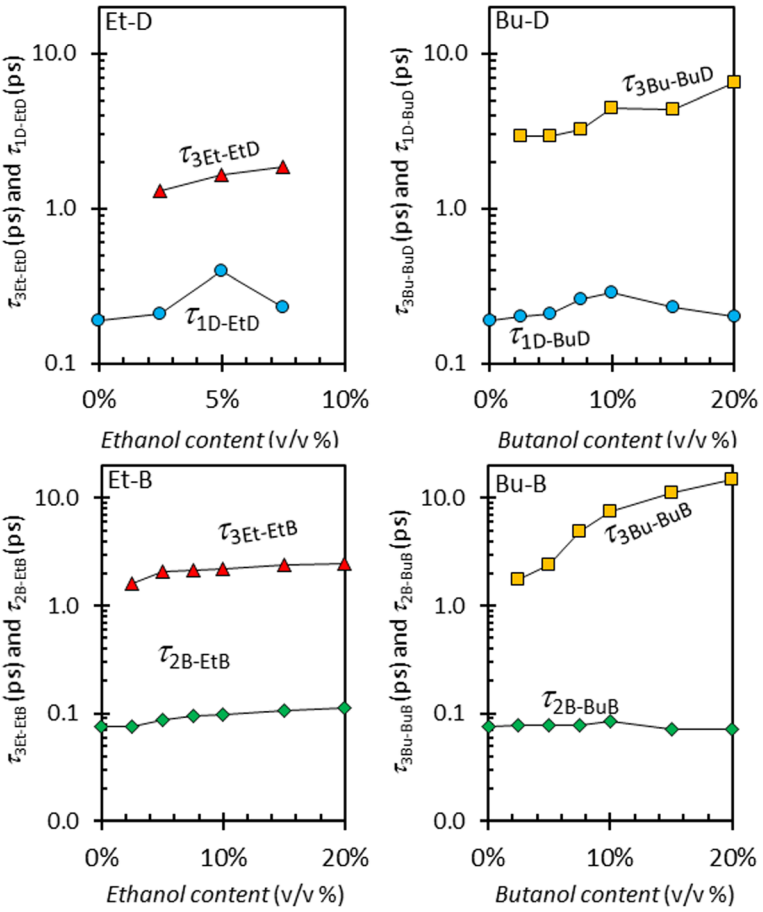

Fig. 3 Fastest relaxation times of the ethanol-diesel (Et-D), ethanol-biodiesel (Et-B), n-butanol-diesel (Bu-D), and n-butanol-biodiesel (Bu-B) blends (≈25 °C)

A second observation is the increase in relaxation time for alcohols in the blends as their concentration is increased. However, as alcohol concentrations increase, the rate of increase in relaxation time decreases. Other authors observed similar trends with different techniques and conditions: Van den Berg et al. [60], with n-butanol in n-hexane; Iglesias et al. [61], with n-pentanol, n-hexanol, and 1-heptanol in n-hexane and cyclohexane; Sato et al. [52], with ethanol in water; and Sagal [62], with ethanol in cyclohexane.

Arik et al. [48], in a similar study with ethanol and gasoline, suggested that this is because the increase in partial volume of ethanol in the mixture provides more space to molecules of alcohol for mobility, which results in longer relaxation time [62]. However, this statement overlooks the fact that the higher availability of space (associated with the increase in excess volume) implies less interaction with surrounding molecules, therefore decreasing the relaxation time. To prove this suggestion, the excess volume was measured for all blends, and the results are shown in Fig. 4. In the figure, for the Et-D system, this relationship is clear: after the initial increase in excess volume, eventually the excess volume decreases with increasing ethanol content; thus, relaxation times increase. For all other systems, however, such a

relationship is not evident. In all these systems (Et-B, Bu-D, and Bu-B), relaxation times increase with the alcohol content, even when the excess volume does not reach its peak. This suggests that the volume factor is not the only factor involved in the dynamic behavior of alcohol molecules in these mixtures, nor is it even the dominant factor, as discussed below.

Comparing both alcohols, it is observed that relaxation times for n-butanol were higher than those for ethanol for analogous blends (same alcohol content), which is related to the size of the molecules [36] (slower relaxation process for larger molecules).

As expected, diesel and biodiesel basically show no variation in relaxation times throughout the frequency range measurement. This is because their dynamics are not linked to the presence of alcohols, at least not significantly for the low concentrations.

The effect of mixing on the fastest dielectric constant contribution for each alcohol ($\varepsilon_{3\text{Et-Et}D}$, $\varepsilon_{3\text{Bu-Bu}D}$, $\varepsilon_{3\text{Et-Et}B}$, and $\varepsilon_{3\text{Bu-Bu}B}$) and for each base fuel ($\varepsilon_{1D\text{-Et}D}$, $\varepsilon_{1D\text{-Bu}D}$, $\varepsilon_{2B\text{-Et}B}$, and $\varepsilon_{2B\text{-Bu}B}$) as a function of alcohol content is shown in Fig. 5. This provides insights into the intermolecular interactions and molecular rearrangement in the mixtures. As already explained for the relaxation times, the fastest dielectric constant contribution of ethanol rises from 2.83 in pure form to 15.00 in the 2.5% (v/v) blend in diesel and up to 14.31 in the 2.5% (v/v) blend in biodiesel. Similarly, n-butanol rises from 2.38 in the pure state to 9.25 in the 2.5% (v/v) blend in diesel and up to 3.85 in the 2.5% (v/v) blend in biodiesel. Nevertheless, in all cases, as the alcohol content increases, the contribution of the fastest dielectric constant ($\varepsilon_{3\text{alc-alc.bf}}$) to the total dielectric constant ($\varepsilon_{\text{alc-alc.bf}}$) decreases. This is a consequence of the previously described effect on the relaxation time: the OH moiety of the molecule passes from a state in which its movements are very restricted by the hydrogen bonds in pure alcohols to a very diluted state, which facilitates its rotation while significantly contributing to macroscopic polarization. It can also be observed that this effect is associated with the size of the alcohol molecule, because under the same conditions and with the same base fuel, the effect of the increase in ethanol content is higher than that of increasing n-butanol content. Note that the increase in the contribution to total dielectric constant from the fastest relaxation event for both alcohols in biodiesel ($\varepsilon_{3\text{alc-}B}$) is lower than that with diesel ($\varepsilon_{3\text{alc-}D}$). Again, this can be explained by the fact that biodiesel has a significant number of centers of high negative charge (unsaturations and oxygen atoms), which may serve as anchors to form H-bonds.

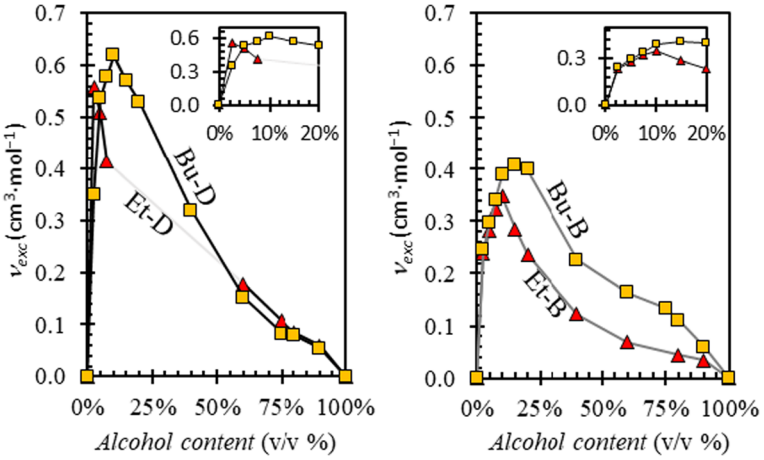

Fig. 4 Excess molar volume for ethanol-diesel (Et-D) and n-butanol-diesel (Bu-D) (left) and ethanol-biodiesel (Et-B) and n-butanol-biodiesel (Bu-B) blends (right)

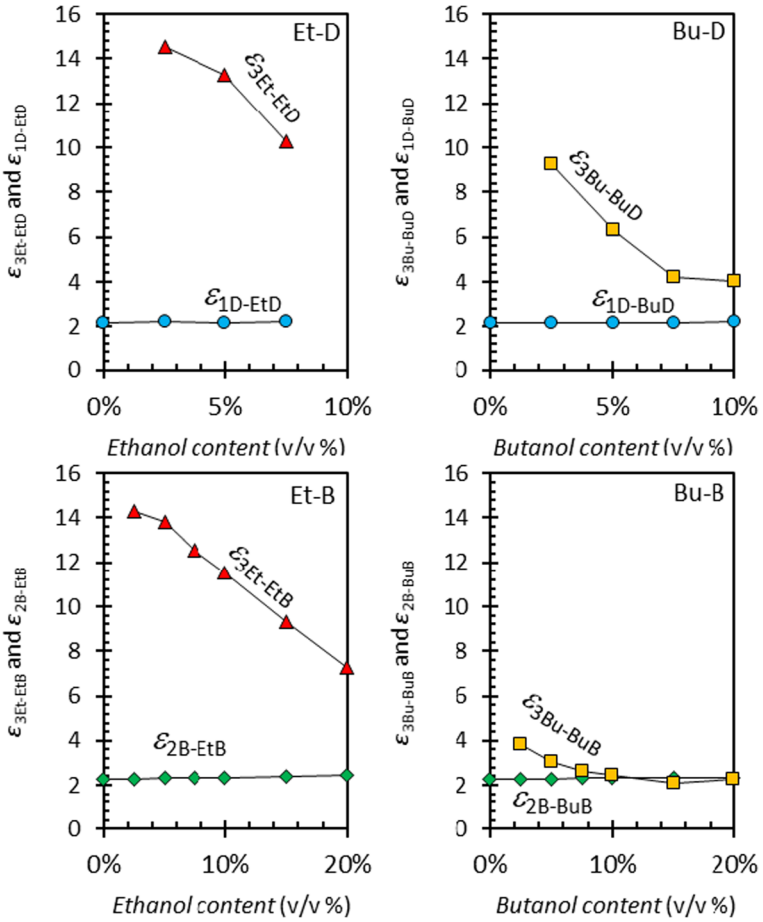

Fig. 5 Dielectric constants of the fastest relaxation event in the ethanol-diesel (Et-D), ethanol-biodiesel (Et-B), n-butanol-diesel (Bu-D), and n-butanol-biodiesel (Bu-B) blends

3.3 Excess Complex Dielectric Constant

The effect of the mixing on the dielectric constant can be observed comparing modeled results for the blends (those for which modeling was possible) with respect to the ideal complex dielectric constant, calculated from the contribution of its components (also modeled), according to the formal definition by Iglesias and Reis [63]. The excess complex dielectric constant, $\varepsilon_{exc}(\omega)$, is defined as the difference between the experimental dielectric constant and the ideal one. However, for a better analysis the modeled dielectric constant, $\varepsilon_{mod}(\omega)$, has been used instead:

$$\varepsilon_{exc}(\omega) = \varepsilon_{mod}(\omega) - \sum_j^n z_j . \varepsilon(\omega)_j \tag{8}$$

where z_j is the volume fractions and $\varepsilon_{exc}(\omega)_j$ is each of the value of the components at the angular frequency ω. The ideal complex dielectric constant of liquid mixtures is a volume-fraction-weighted average of the pure components [64]. This equation was used by Kanyathare et al. [16] to study the adulteration of diesel fuel with kerosene.

It is well known that excess dielectric constant (ε_{exc}) provides qualitative information about the interaction of molecules [65] on the formation or extinction of resonant centers (also called multimers). If $\varepsilon_{exc} = 0$, the components of the blend do not interact with each other, and therefore, each component maintains its resonating poles. Negative values imply that the components of the mixture interact in such a way that the number of effective resonant poles (multimers) is reduced and the opposite occurs for $\varepsilon_{exc} > 0$ [66]. Furthermore, Iglesias et al. [67] proposed that the excess values have three separate contributions. The first contribution is the volume change by the mixing, ε_{exc}[volume], related to excess molar volume according to Eq. 9. The second contribution is the contrast of dielectric constant between the components of the mixture, ε_{exc}[contrast], which is a strong function of the dielectric constant of the components of the mixture and their composition, according to Eq. 10. The third contribution, ε_{exc}[interactions], is due to changes in the interactions of the molecules in the mixture. In practice, the latter is estimated by the difference between the real part of the dielectric constant and the two other contributions, such as expressed in Eq. 11:

$$\varepsilon_{exc}(\omega)^{volume} = -\frac{\nu_{exc}}{\nu}[\varepsilon_{ideal}(\omega)-1] \tag{9}$$

$$\varepsilon_{exc}(\omega)^{contrast} = -\varepsilon_{real\ bf}(\omega) * \frac{z_{alc} * (1-z_{alc}) * \left(r_{alc/bf}-1\right)^2}{r_{alc/bf} + 2 + z_{alc} * \left(r_{alc/bf}-1\right)} \tag{10}$$

$$\varepsilon_{exc}(\omega)^{interactions} = \varepsilon_{real-exc}(\omega) - \varepsilon_{exc}(\omega)^{volume} - \varepsilon_{exc}(\omega)^{contrast} \tag{11}$$

where ν is the molar volume and $r_{alc/bf}$ is the permittivity contrast of the mixture, defined as the ratio $\varepsilon_{real\ alc}(\omega)/\varepsilon_{real\ bf}(\omega)$.

Since the dielectric constants are highly frequency dependent (which is characteristic of relaxation processes), their excess values are also highly frequency dependent. However, for the purpose of the following analysis, the average of the real part (as well as its three contributions, volume, contrast, and interactions) and of the imaginary part of the dielectric constant were taken, in the range of approximately 0.10 and 1.10 THz, and represented against the alcohol content. The results obtained are shown in Fig. 6.

Comparing Fig. 6 with Fig. 4, it can be noted that there is no apparent correlation between the excess molar volume (always positive) and the excess of the real components of the dielectric constant. This would suggest that volume is not the predominant contribution in the dynamic behavior of these systems, as mentioned in the previous section, and in agreement with Iglesias et al. [67], who suggested that the contribution of excess volume is usually small and has a minor influence. In addition, it is also observed that the contrast contribution is also small, despite the components of the mixtures having differences from a polarity standpoint. In general, the model indicates that the interactions constitute the main contribution to explain the behavior of $\varepsilon_{real\ exc}$.

As a whole, the $\varepsilon_{real\text{-}exc}$ for Et-B and Bu-B is negative. It suggests that the energy stored per unit volume by this system is less than the ideal system would be, possibly because coupling occurs in such a way that the number of resonant dipoles, which contributes to the dielectric polarization of the mixture, is reduced [22]. The same applies to Et-D with the exception for very low concentrations. The Bu-B system behaves very closely to ideal.

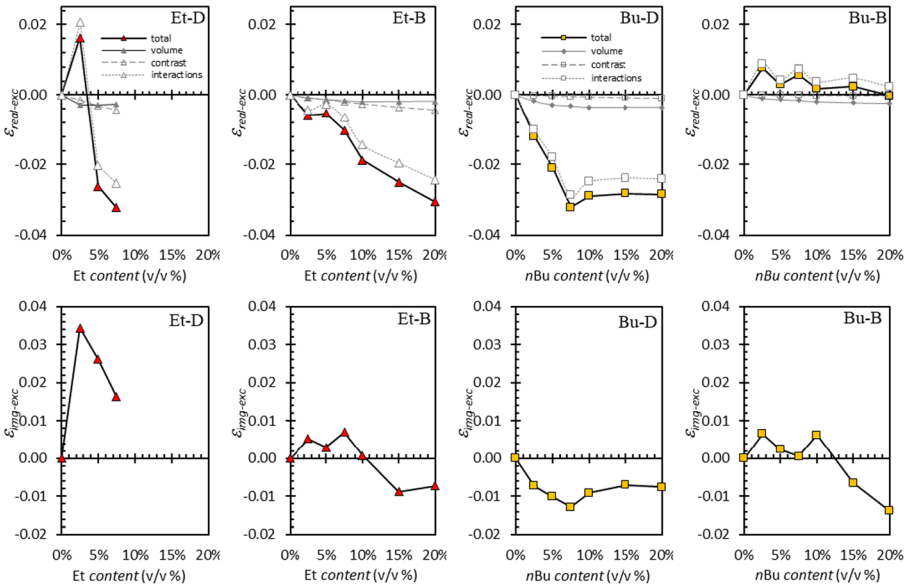

Fig. 6 Excess of real part (top) of dielectric constant showing their contributions (volume, contrast, and interactions) and excess of imaginary part (bottom) of the dielectric constant against the content of alcohol, for ethanol-diesel (Et-D), ethanol-biodiesel (Et-B), n-butanol-diesel (Bu-D), and n-butanol-biodiesel (Bu-B) blends

The excess of the imaginary part of the complex dielectric constant of the blends ($\varepsilon_{img\text{-}exc}$) are shown in Fig. 6, bottom. The excess of the imaginary part becomes positive for Et-D, negative for Bu-D blends, and alternating for Et-B and Bu-B blends (positive at the lowest concentrations and negative for alcohol contents higher than 10%). The behavior of the Et-D system could be interpreted because the formed dipoles align more slowly to follow the oscillating field (E) than they would in the ideal mixture. This is consistent with the increasing relaxation time of alcohols at these concentrations, as outlined in Section 3.2. For the Bu-D system, the opposite behavior occurs: the formed dipoles are aligned faster to follow the oscillating field (E) than in the ideal mixture. The Bu-B and Et-B systems have a behavior very close to ideality.

Dielectric losses are usually described by the tangent of the loss angle, tan δ, which is the ratio between the imaginary and real parts of the complex dielectric constant (tan $\delta=\varepsilon_{img}/\varepsilon_{real}$). The ratio tan δ/tan δ [ideal] is a measure of the difference between the real and ideal behavior. This ratio was estimated for all the studied systems, and the results are shown in Fig. 7. From this figure, it can be observed that for system Et-D, tan δ is higher than the ideal one. This means that there is a higher delay in the response time to the electric field than ideally. For the Bu-D blends, the opposite is observed; i.e., the system responds faster to the electric field than ideally. Finally, Et-B and Bu-B systems respond similarly to an ideal system. This behavior is consistent with the behavior of ε_{img}.

The results of this study are subject to limitations derived from the assumptions made. In addition to being a technique with a relatively short path, most of the published studies on mixtures are reduced to binary systems. To the authors' knowledge, only a few of them address mixtures with more than two components [47, 48, 56, 68]. It is clear that the application of the technique to samples of such complexity, such as diesel fuel and biodiesel, is a challenge. The extension of the reasoning used for binary mixtures to systems with many

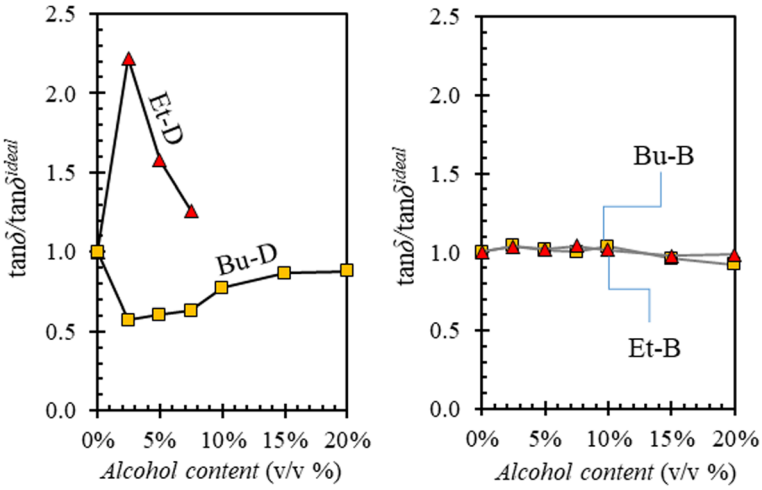

Fig. 7 Ratio of the loss angle tangent of alcohol-diesel mixtures (left) and biodiesel mixtures (right) relative to ideal loss angle

more components is not directly applicable for intermolecular interactions. For example, the consideration that only the fastest relaxation processes are significant for alcohols, assuming that the two slowest ones (cooperative volume relaxation and rotation of one end of the chain or of a free alcohol molecule) remain constant, is arguable for high alcohol contents, where interactions between alcohol molecules start to be important. Furthermore, a better interpretation of the results, in particular those related to the excess of dielectric constant, requires information on the thermodynamic processes associated with the mixing, such as mixing enthalpy, an indicator of the generation and breakdown of intermolecular H-bonds during the mixing process [52, 59].

In complex mixtures, much more information is required to estimate, more accurately, how the alcohol content affects the molecular dynamics, the molecular interactions, and, consequently, the properties depending on them. In this respect, experiments could be designed with a diesel surrogate, in which the relative concentrations of its main components are systematically modified, until a full and realistic picture of the molecular interactive phenomena is outlined.

4 Conclusions

The real and imaginary excess of dielectric constant, for pure fuels and binary blends of alcohol (ethanol and n-butanol) and commercial fuels (diesel and biodiesel), were determined and analyzed starting from the spectra in the time-domain in the terahertz frequency region at room temperature. The main conclusions are:

1. The complex dielectric constant of pure components was successfully modeled with a single Debye model for diesel, double for biodiesel, and triple for ethanol and n-butanol. With regard to blends, the systems studied could not be fitted along the whole mixing range, but only for concentrations up to 7.5% (v/v) for Et-D blends and up to 20% (v/v) for Bu-D, Et-B, and Bu-B blends.

2. The faster relaxation time of both alcohols was found to be significantly higher for low alcohol contents than for pure alcohols. However, such increase was higher as the alcohol content was increased in the sample within the fitted low concentration range. The effect of the alcohol content on the faster relaxation time was much lower for diesel and biodiesel.
3. Similarly, as with the relaxation time, the contribution of the dielectric constant value by the faster relaxation event increased significantly more for low alcohol contents than for pure alcohol. However, successive increases of alcohol content led to lower contribution, following an asymptotic tendency (within the fitted low concentration range).
4. Ethanol takes the blends further away from the ideal behavior than n-butanol does. The blends that held the most ideal behavior were those with n-butanol. This suggests that the length of the carbon chain of alcohol plays an important role, either because it provides inertia to the molecules or because it contributes to increase the low-energy molecular interactions.
5. Among the three types of contributions for the dielectric constant excess, it has been found that the volume and contrast contributions are relatively small and maybe negligible in front of the contribution of interactions, to explain the dynamic behavior of the studied systems.
6. The study of the ratio of the loss angle tangent to the ideal suggests that systems with biodiesel tend to behave closer to the ideal than the systems with diesel fuel.

It would be worthwhile in future works to expand the frequency range to include lower frequencies to ensure accurate determination of relaxation times, as well as to evaluate the effect of temperature, since the relaxation processes are highly sensitive to this variable. Similarly, studies with neat paraffins (such as n-hexadecane) and methyl esters (such as methyl decanoate) would be helpful to avoid the complexity of diesel and biodiesel and could therefore generate a better understanding of the mechanisms responsible for relaxation processes. Finally, mixtures with high ethanol content need to be tested using an inert gas facility (a N_2 chamber, for instance) to reduce the uncertainties caused by the high degree of fluctuation due to the humidity in these samples.

Nomenclature *A,* Amplitude; *CFPP,* Cold filter plugging point; *d,* Thickness of the sample; *E,* Electric field; *f,* Oscillator strength; *FFT,* Fast Fourier transform; *I,* Intensity; *k,* Extinction coefficient; *MSD,* Mean squared deviation; *n,* Refraction index; *r,* Permittivity contrast; *t,* Time; *tan δ,* Tangent of the loss angle; *TDS,* Time-domain spectroscopy; *THz,* Terahertz; *z,* Volume fractions; α, Absorption coefficient; α, Asymmetry parameter of the *Havriliak-Negami relaxation model;* β, Broadness parameter of the *Havriliak-Negami relaxation model;* ε, Dielectric constant; γ_L, Damping constant; θ, Phase; τ, Relaxation time; ν, Molar volume; ω, Angular frequency

Subscripts *alc,* Alcohol; *B,* Biodiesel; *bf,* Base fuel; *Bu,* N-Butanol; *D,* Diesel fuel; *Et,* Ethanol; *exc,* Excess; *img,* Imaginary part; *j,* Sample index; *mod,* Modeled; *real,* Real part; *ref,* Reference

Acknowledgements Repsol is acknowledged as a supplier of diesel fuel, Bio Oils for the donation of biodiesel fuel, Abengoa Bioenergy for the donation of ethanol, and Green Biologics Ltd. for the donation of n-butanol. T.P. Iglesias appreciates the financial support ED431C 2016-034 provided by the Xunta de Galicia (Spain).

Funding Open Access funding provided thanks to the CRUE-CSIC agreement with Springer Nature.

References

1. Wheals, A.E.; Basso, L.C.; Alves, D. M.; Amorim, H.V. Fuel ethanol after 25 years. *Trends Biotechnol*, **1999,** *17* (12), 482-487. doi:https://doi.org/10.1016/S0167-7799(99)01384-0.
2. Da Silva Trindade, W.R.; Gonçalves dos Santos, R. Review on the characteristics of butanol, its production and use as fuel in internal combustion engines. *Renewable Sustainable Energy Rev.*, **2017,** *69*, 642-651. doi: https://doi.org/10.1016/j.rser.2016.11.213.
3. Çelebi, Y; Aydin, H. An overview on the light alcohol fuels in diesel engines*, Fuel,* **2019**, *236*, 890-911. doi: https://doi.org/10.1016/j.fuel.2018.08.138.
4. Maiti, S.; Gallastegui, G.; Sarma, S.J.; Brar, S.K.; Bihan, Y.L.; Drogui, P.; Buelna G.; Verma, M. A re-look at the biochemical strategies to enhance butanol production, *Biomass Bioenergy*, **2016**, *94*, 187-200. doi: https://doi.org/10.1016/j.biombioe.2016.09.001.
5. Ndaba, B.; Chiyanzu, I.; Marx, S. n-Butanol derived from biochemical and chemical routes: A review. *Biotechnol. Rep,* **2015**, *8*, 1–9. doi: https://doi.org/10.1016/j.btre.2015.08.001.
6. Lapuerta, M.; García-Contreras, R.; Campos-Fernández, J.; Dorado, M.P. Stability, lubricity, viscosity, and cold-flow properties of alcohol-diesel blends, *Energy Fuels*, **2010**, *24*, 4497-4502. doi: https://doi.org/10.1021/ef100498u.
7. Lapuerta, M.; Rodríguez-Fernández, J.; Fernández-Rodríguez, D.; Patiño-Camino, R. Cold flow and filterability properties of n-butanol and ethanol blends with diesel and biodiesel fuels*, Fuel,* 2018, *224* (15), 552-559. doi: https://doi.org/10.1016/j.fuel.2018.03.083.
8. Jin, C.; Zhang, X.; Han, W.; Geng, Z.; Thomas, M.; Jeffrey, A.; Wang, G.; Ji, J.; Liu, H. Macro and micro solubility between low-carbon alcohols and rapeseed oil using different co-solvents*, Fuel,* **2020**, *270*, 117511. doi: https://doi.org/10.1016/j.fuel.2020.117511.
9. Zaharin, M.; Abdullah, N.; Najafi, G.; Sharudin, H.; Yusaf, T. Effects of physicochemical properties of biodiesel fuel blends with alcohol on diesel engine performance and exhaust emissions: A review, *Renewable Sustainable Energy Rev.*, **2017,** *79*, 475-493. doi: https://doi.org/10.1016/j.rser.2017.05.035.
10. Kumar, S.; Hyun Cho, J.; Park, J. Advances in diesel–alcohol blends and their effects on the performance and emissions of diesel engines. *Renewable Sustainable Energy Rev.*, **2013,** *22*, 46-72. doi: https://doi.org/10.1016/j.rser.2013.01.017.
11. Lennox, S.; Lukács, K.; Torok, A.; Akos, B.; Mbarawa, M.; Penninger, A.; Kolesnikov, A. Combustion and emission characteristics of n-butanol/diesel fuel blend in a turbo-charged compression ignition engine. *Fuel*, **2013**, *107*, 409-418. doi: https://doi.org/10.1016/j.fuel.2012.11.083.
12. Wu, Y.; Zhang, X.; Zhang, Z.; Wang, X.; Geng, Z.; Jin, C.; Liu, H.; Yao, M. Effects of diesel-ethanol-THF blend fuel on the performance and exhaust emissions on a heavy-duty diesel engine*, Fuel,* **2020**, *271*, 117633. doi: https://doi.org/10.1016/j.fuel.2020.117633.
13. Corach, J.; Colman, M.; Sorichetti, P.; Romano, S. Kinematic viscosity of soybean biodiesel and diesel fossil fuel blends: Estimation from permittivity and temperature*, Fuel,* **2017**, *207*, 488-492. doi: https://doi.org/10.1016/j.fuel.2017.06.102.
14. Zhao, H.; Zhao, K.; Bao, R. Predicting Cold Flow Properties of Diesel by Terahertz Time-Domain Spectroscopy. *ISRN*, **2012**, 1-4. doi:https://doi.org/10.5402/2012/876718.
15. Eskinera, M.; Ammer, F.; Then, D.; Staufenbiel, J.; Rossner, M.; Schröder, O.; Krahl, J. Novel concepts for onboard determination of fuel quality in plug-in hybrid cars. *Fuel*, **2017**, *209*, 224-231. doi: https://doi.org/10.1016/j.fuel.2017.07.102.
16. Kanyathare, B.; Asamoah, B.; Peiponen, K.-E. Imaginary optical constants in near-infrared (NIR) spectral range for the separation and discrimination of adulterated diesel oil binary mixtures. *Opt. Rev.*, **2019**, *26*, 85-94. doi:https://doi.org/10.1007/s10043-018-0481-9.

17. Abdul-Munaim, A.; Reuter, M.; Abdulmunem, O.; Balzer, J.; Koch, M. Using Terahertz Time-Domain Spectroscopy to discriminate among water contamination levels in diesel Engine Oil. *Trans ASAB*, *59.*, **2016** *3*, 795-801. doi: https://doi.org/10.13031/trans.59.11448.
18. Campos, D.; Dall'Oglio, E.; De Sousa Jr. P.; Vasconcelos, L.; Kuhnen, C. Investigation of dielectric properties of the reaction mixture during the acid-catalyzed transesterification of Brazil nut oil for biodiesel production. *Fuel.*, **2014,** *117*, 957-965. doi: https://doi.org/10.1016/j.fuel.2013.10.037.
19. Debye, P. J. W. Polar Molecules; The Chemical Catalog Co., Inc., New York **1929**.
20. Lee, Y.-S. Principles of Terahertz Science and Technology, Springer, Ed., Corvallis, **2009**. ISBN: 978-0-387-09540-0.
21. Onimisi, M.Y.; Ikyumbur, J.T. Comparative Analysis of Dielectric Constant and Loss Factor of Pure Butan-1-ol and Ethanol. *Am. J. Condens. Matter Phys*, **2015,** *5(3)*, 69-75. doi: https://doi.org/10.5923/j.ajcmp.20150503.02
22. Mehrotra, S. C.; Kumbharkhane, A.; Chaudhari, A. Binary Polar Liquids: Structural and Dynamic Characterization Using Spectroscopic Methods (first ed.). **2017**. Elsevier. doi: https://doi.org/10.1016/B978-0-12-813253-1.00001-X.
23. Cole, K.S.; Cole, R.H. Dispersion and absorption in dielectrics I. *J. Chem. Phys.*, **1941,** *9*(341), 341-351. doi: https://doi.org/10.1063/1.1750906.
24. Davidson, D.W.; Cole, R.H. Dielectric Relaxation in Glycerol, Propylene Glycol, and nPropanol. *J. Chem. Phys.*, **1951**, *19*(12), 1484-1490. doi:https://doi.org/10.1063/1.1748105.
25. Havriliak, S.; Negami, S. A complex plane representation of dielectric and mechanical relaxation processes in some polymers. *Polymer*, **1967**, *8*, 161-210. doi: https://doi.org/10.1016/0032-3861(67)90021-3.
26. Sarkar, S.; Saha, D.; Banerjee, S.; Mukherjee, A.; Mandal, P. Broadband terahertz dielectric spectroscopy of alcohols. *Chem. Phys. Lett.*, **2017**, *678*, 65-71. doi: https://doi.org/10.1016/j.cplett.2017.04.026.
27. Yomogida, Y.; Sato, Y.; Nozaki, R.; Mishina, T.; Nakahara, J. Dielectric study of normal alcohols with THz time-domain spectroscopy. *J. Mol. Liq.*, **2010**, *154*, 31-35. doi: https://doi.org/10.1016/j.molliq.2010.03.007.
28. Fukasawa, T.; Sato, T.; Watanabe, J.; Hama, Y.; Kunz, W.; Buchner, R. Relation between Dielectric and Low-Frequency Raman Spectra of Hydrogen-Bond Liquids. *Phys. Rev. Lett.*, **2005,** *95*, 197802. 1-4. doi: https://doi.org/10.1103/PhysRevLett.95.197802.
29. Kindt, J.T.; Schmuttenmaer, C.A. Far-Infrared Dielectric Properties of Polar Liquids Probed by Femtosecond Terahertz Pulse Spectroscopy. *J. Phys. Chem.*, **1996,** *100*(24), 10373-10379. doi:https://doi.org/10.1021/jp960141g.
30. Lukichev, A. Relaxation function for the non-Debye relaxation spectra description. *Chem. Phys.*, **2014,** *428*, 29-33. doi: https://doi.org/10.1016/j.chemphys.2013.10.021.
31. Hill, R.; Dissado, L. Debye and non-Debye relaxation. *J. Phys. C: Solid State Phys.*, **1985,** *18*, 3829-3836. Doi: https://doi.org/10.1088/0022-3719/18/19/021.
32. Feldman, Y.; Puzenko, A.; Ryabov, Y. Non-Debye dielectric relaxation in complex materials. *Chem. Phys.*, **2002**, *284*, 139–168. doi: https://doi.org/10.1016/S0301-0104(02)00545-1.
33. Dai, X.; Fan, S.; Qian, Z.; Wang, R.; Wallace, V.P.; Sun, Y. Prediction of the terahertz absorption features with a straightforward molecular dynamics method, *Spectrochim. Acta, Part A*, **2020,** *236*, 118330. doi: https://doi.org/10.1016/j.saa.2020.118330.
34. Shilov, I. Molecular dynamics simulation of dielectric constant and cluster structure of liquid methanol: the role of cluster-cluster dipole correlations, *Mol. Phys.*, **2015**, *113*(6), 570-576. doi: https://doi.org/10.1080/00268976.2014.960496.
35. Elton, D.C. The origin of the Debye relaxation in liquid water and fitting the high frequency excess response. Phys. Chem., **2017**, *28*, 18739-18749. doi: https://doi.org/10.1039/C7CP02884A.
36. El Khaled, D.; Novas, N.; Gázquez, J. A.; García, R. M.; Manzano-Agugliaro, F. Alcohols and alcohols mixtures as liquid biofuels: A review of dielectric properties. *Renewable Sustainable Energy Rev.*, **2016,** *66*, 556-571. doi: https://doi.org/10.1016/j.rser.2016.08.032.
37. Li, R.; D'Agostino, C.; McGregor, J.; Mantle, M.; Zeitler, J. Mesoscopic structuring and dynamics of alcohol/water solutions probed by terahertz time-domain spectroscopy and pulsed field gradient nuclear magnetic resonance. *J. Phys. Chem. B*, **2014**, *118*(34), 10156-10166. doi:https://doi.org/10.1021/jp502799x.
38. Zasetsky, A.; Buchner, R. Quasi-linear least squares and computer code for numerical evaluation of relaxation time distribution from broadband dielectric spectra. *J. Phys.: Condens. Matter.*, **2011,** *23*, 1-8. doi: https://doi.org/10.1088/0953-8984/23/2/025903.
39. Florsch, N.; Revil, A.; Camerlynck, C. Inversion of generalized relaxation time distributions with optimized damping parameter. *J. Appl. Geophys.*, **2014**, *1069*, 119-132. doi: https://doi.org/10.1016/j.jappgeo.2014.07.013.
40. Barthel, J.; Buchner, R. High frequency permittivity and its use in the investigation of solution properties. *Pure Appl. Chem.*, **1991**, *63*(10), 1473-1482. doi: https://doi.org/10.1351/pac199163101473.
41. Beneduci, A. Which is the effective time scale of the fast Debye relaxation process in water? *J. Mol. Liq.*, **2008**, *138*, 55-59. doi: https://doi.org/10.1016/j.molliq.2007.07.003.

42. Lapuerta, M.; Rodríguez Fernández, J.; Patiño-Camino, R.; Cova-Bonillo, A.; Monedero, E.; Meziani, Y.M. Determination of optical and dielectric properties of blends of alcohol with diesel and biodiesel fuels from terahertz spectroscopy. *Fuel*, **2020**, *274* (117877), 1-7. doi: https://doi.org/10.1016/j.fuel.2020.117877.
43. Ji, T.; Zhang, Z.; Zhao, H.; Chen, M.; Yu, X.; Xiao, T. A THz-TDS measurement method for multiple samples. *Opt. Commun.*, **2014,** *312*, 292–295. doi: https://doi.org/10.1016/j.optcom.2013.09.013.
44. Jin, C.; Pang, X.; Zhang, X.; Wu, S.; Ma, M.; Xiang, Y. et al. Effects of C3–C5 alcohols on solubility of alcohols/diesel blends*, Fuel,* **2019**, *236*, 65-74. doi: https://doi.org/10.1016/j.fuel.2018.08.129.
45. Bilgin, A.; Durgun, O.; Sahin, Z. The Effects of Diesel-Ethanol Blends on Diesel Engine Performance. *Energy Sources*, **2002**, *24*, 431-440. doi: https://doi.org/10.1080/00908310252889933.
46. Lapuerta, M.; Hernández, J.; Fernández-Rodríguez, D.; Cova-Bonillo, A. Autoignition of blends of n-butanol and ethanol with diesel or biodiesel fuels in a constant-volume combustion chamber. *Energy*, **2017,** *118*(1), 613-621. doi: https://doi.org/10.1016/j.energy.2016.10.090.
47. Arik, E.; Altan, H.; Esenturk, O. Dielectric Properties of Diesel and Gasoline by Terahertz Spectroscopy. *J Infraed Millim Te*, **2014,** *35*(9), 759-769. doi: https://doi.org/10.1007/s10762-014-0081-0.
48. Arik, E.; Altan, H.; Esenturk, O. Dielectric Properties of Ethanol and Gasoline Mixtures by Terahertz Spectroscopy and an Effective Method for Determination of Ethanol Content of Gasoline. *J. Phys. Chem. A*, **2014**, *118*(17), 3081-3089. doi: https://doi.org/10.1021/jp500760t.
49. Zhang, X.; Xu, J. Introduction to THz wave photonics (first ed.), Springer, New York. **2010**. ISBN: 978-1-4419-0978-7.
50. Hasted, J.; Husain, S.; Frescura, F., Birch, J. Far-infrared absorption in liquid water. *Chem. Phys. Lett.*, **1985**, *118*(6), 98-105. doi: https://doi.org/10.1016/j.trac.2012.11.009.
51. Flanders, B.; Cheville, R.; Grischkowsky, D.; Scherer, N. Pulsed Terahertz Transmission Spectroscopy of Liquid CHCl3, CCl4, and their Mixtures. *J. Phys. Chem.* , **1996,** *100*(29), 11824-11835. doi: https://doi.org/10.1021/jp960953c.
52. Sato, T. Dielectric Relaxation Processes in Ethanol/Water Mixtures. *J. Phys. Chem. A*, **2004,** *108*, 5007-5015. doi:https://doi.org/10.1021/jp035255o.
53. Møller, U.; Cooke, D.; Tanaka, K.; Jepsen, P. Terahertz reflection spectroscopy of Debye relaxation in polar liquids. *J. Opt. Soc. Am. B: Opt. Phys.*, **2009,** *29*(9), A113-A125. doi:https://doi.org/10.1364/JOSAB.26.00A113.
54. Mittleman, D.M.; Nuss, M.C.; Colvin, V.L. Terahertz spectroscopy of water in inverse micelles. *Chem. Phys. Lett.*, **1997,** *275*, 332-338. doi: https://doi.org/10.1016/S0009-2614(97)00760-4.
55. Gabriel, C.; Gabriel, S.; Grant, E.; Halstead, B.; Mingos, D. Dielectric parameters relevant to microwave dielectric heating. Chemical Society Reviews, **1998,** *27*, 213-224. doi: https://doi.org/10.1039/A827213Z.
56. Vralstad, H; Spets, Ø.; Lesaint, C.; Lundgaard, L.; Sjöblom, J. Dielectric Properties of Crude Oil Components. *Energy Fuels*, **2009,** *23*, 5596–5602. doi: https://doi.org/10.1021/ef900445n.
57. Lou, J.; Hatton, T.; Laibinis, P.E. Effective Dielectric Properties of Solvent Mixtures at Microwave Frequencies. *J. Phys. Chem. A*, **1997,** *101*, 5262-5268. doi:https://doi.org/10.1021/jp970731u.
58. Chmielewska, A.; Zurada, M.; Klimaszewski, K.; Bald, A. Dielectric Properties of Methanol Mixtures with Ethanol, Isomers of Propanol, and Butanol. *J. Chem. Eng. Data*, **2009**, *54*(3), 801-806. doi:https://doi.org/10.1021/je800593p.
59. Reis, J.; Iglesias, T.; Douhéret, G.; Davis, M. The permittivity of thermodynamically ideal liquid mixtures and the excess relative permittivity of binary dielectrics. *Chem. Phys.*, **2009**, *11*, 3977-3986. doi: https://doi.org/10.1039/B820613A.
60. Van den Berg, J.; Michielsen, J.; Ketelaar, J. Dielectric properties of 1-butanol and of mixtures of 1-butanol with hexane and with tetrachloromethane. Recueil des Travaux Chimiques des Pays-Bas, **1974**, *95*(4), 104-107. doi: https://doi.org/10.1002/recl.19740930404.
61. Iglesias, T.; Forniés-Marquin, J.; De Cominges, B. Excess permittivity behaviour of some mixtures n-alcohol + alkane: an interpretation of the underlying molecular mechanism. *J. Chem. Phys*, **2005,** *103*(19), 2639-2646. doi:https://doi.org/10.1080/00222930500190384.
62. Sagal, M.W. Dielectric Relaxation in Liquid Alcohols and Diols. *J. Chem. Phys.*, **1962,** *36*, 2437-2442. doi: https://doi.org/10.1063/1.1732905.
63. Iglesias, T.P.; Reis, J.R. On the definition of the excess permittivity of a fluid mixture. III: Dependence on frequency. *J Chem Thermodym.*, **2016,** *96*, 208-209. doi: https://doi.org/10.1016/j.jct.2015.12.035.
64. Iglesias, T. P.; Reis, J. R. On the importance of ideal properties to understand the dielectric relaxation of liquid mixtures. *J. Mol. Liq.*, **2018,** *264*, 143–149. doi: https://doi.org/10.1016/j.molliq.2018.05.028.
65. Tabellout, M.; Lanceleur, P.; Emery, J.; Hayward, D.; Pethrick, R. Dielectric, ultrasonic and carbon-13 nuclear magnetic resonance relaxation measurements of t-butyl alcohol–water mixtures. *J. Chem. Soc., Faraday Trans.*, **1990**, *9*(86), 1493-1501. doi:https://doi.org/10.1039/FT9908601493.
66. Sengwa, R.; Khatri, V. Study of static permittivity and hydrogen bonded structures in amide–alcohol mixed solvents. *Thermochim. Acta*, **2010**, *506*, 47-51. doi: https://doi.org/10.1016/j.tca.2010.04.013.

67. Iglesias, T.P.; Reis, J.R. Separating the contributions of the volume change upon mixing, permittivity contrast and molecular interactions in the excess relative permittivity of liquid mixtures. *Chem. Phys.*, **2015**, *17*, 13315-13322. doi: https://doi.org/10.1039/c4cp05987e.
68. Lesaint, C.; Simon, S.; Lesaint, C.; Glomm, W.; Berg, G.; Lundgaard, L.; Sjöblom, J. Dielectric Properties of Asphaltene Solutions: Solvency Effect on Conductivity. *Energy Fuels*, **2013,** 27, 75-81. doi:https://doi.org/10.1021/ef3013129.